Journal of Cardiovascular Computed Tomography 13 (2019) 118–127

Contents lists available at ScienceDirect

Journal of Cardiovascular Computed Tomography

journal homepage: www.elsevier.com/locate/jcct

Analysis of the anatomical features of pulmonary veins on pre-procedural cardiac CT images resulting in incomplete cryoballoon ablation for atrial fibrillation

Yoriaki Matsumoto[a,b,*], Yuji Muraoka[c], Yoshinori Funama[d], Shinji Mito[c], Takanori Masuda[a,b], Tomoyasu Sato[e], Tomoyuki Akita[f], Kazuo Awai[b]

[a] Department of Radiological Technology, Tsuchiya General Hospital, 3-30 Nakajima-cho, Naka-ku, Hiroshima, 730-8655, Japan
[b] Department of Diagnostic Radiology, Graduate School of Biomedical and Health Sciences, Hiroshima University, 1-2-3 Kasumi, Minami-ku, Hiroshima, 734-8551, Japan
[c] Department of Cardiology, Tsuchiya General Hospital, 3-30 Nakajima-cho, Naka-ku, Hiroshima, 730-8655, Japan
[d] Department of Medical Physics, Faculty of Life Sciences, Kumamoto University, 4-24-1 Kuhonji, Kumamoto, 862-0976, Japan
[e] Department of Radiology, Tsuchiya General Hospital, 3-30 Nakajima-cho, Naka-ku, Hiroshima, 730-8655, Japan
[f] Department of Epidemiology, Infectious Disease Control and Prevention, Graduate School of Biomedical and Health Sciences, Hiroshima University, 1-2-3 Kasumi, Minami-ku, Hiroshima, 734-8551, Japan

ARTICLE INFO

Keywords:
Cardiac computed tomography
Atrial fibrillation
Cryoballoon ablation
Pulmonary vein
Anatomical features

ABSTRACT

Background: To investigate the anatomical features related to the failure of cryoballoon (CB) ablation for atrial fibrillation (AF) on pre-procedural CT images.
Methods: We retrospectively analyzed CT images of 100 patients with AF who had undergone a first CB ablation at our institution between June 2016 and April 2017. We measured the angle, short- and long axis length, and the area and ovality of 4 major pulmonary vein (PV) ostium on CT images. We performed logistic regression analysis to analyze the anatomical features related to the failure (incomplete CB ablation) of PV isolation. We also performed a receiver-operating characteristic (ROC) curve analysis to identify an appropriate cut-off value for anatomical features significantly associated with incomplete CB ablation.
Results: We analyzed 400 PVs in 100 patients [aged 64 (range, 27–82) years, 59% male]. The rate of incomplete CB ablation was significantly higher for right-than left-sided PVs ($p < 0.001$). The anatomical feature significantly associated with incomplete CB ablation was the angle at the right inferior PV (RIPV) (AOR: 1.17; 95% CI: 1.09–1.27, $p < 0.001$) and the right superior PV (RSPV) (AOR: 1.12; 95% CI: 1.01–1.23; $p = 0.014$). In the ROC analysis, the optimal cut-off value for RIPV and RSPV angle to discriminate an incomplete CB ablation were 40.1° and 79.7°, respectively.
Conclusion: Our findings may help to select the appropriate ablation strategy to treat patients with AF. We show that the angle is an anatomical feature significantly related to failed CB ablation.

1. Introduction

Atrial fibrillation (AF) is the most common cardiac arrhythmia.[1] It is significantly associated with morbidity and mortality due to stroke and thromboembolism.[2,3] Electrical isolation of pulmonary veins (PVs) by catheter ablation is the standard approach to treat AF.[4,5] Although radiofrequency (RF) catheter ablation is the established treatment for AF, cryoballoon (CB) ablation is a promising alternative to achieve PV isolation. With CB ablation it is possible to obtain circumferential PV isolation in a single procedure. Therefore, the procedure time is shorter and the risk for thermal injury and PV stenosis are lower than with RF ablation.[6–8] In a recently multicenter randomized trial, CB- was not inferior to RF ablation in patients with paroxysmal AF (1-year Kaplan-Meier event rate estimates 34.6% and 35.9%, respectively; $p < 0.001$

Abbreviations: AF, Atrial fibrillation; AOR, adjusted odds ratio; AUC, area under the curve; CB, cryoballoon; CI, confidence interval; CNR, contrast-to-noise ratio; FOV, field of view; HU, Hounsfield Units; LA, left atrium; LAA, left atrial appendage; LIPV, left inferior pulmonary vein; LSPV, left superior pulmonary vein; LV, left ventricle; MPR, multiplanar reconstruction; PV, pulmonary vein; RA, right atrium; RF, radiofrequency; RIPV, right inferior pulmonary vein; ROC, receiver-operating characteristic; ROI, region of interest; RSPV, right superior pulmonary vein; SD, standard deviation; 3D, 3-dimensional

* Corresponding author. Department of Radiological Technology, Tsuchiya General Hospital, 3-30 Nakajima-cho, Naka-ku, Hiroshima, 730-8655, Japan.
E-mail address: yori_8592_8592@yahoo.co.jp (Y. Matsumoto).

https://doi.org/10.1016/j.jcct.2018.11.005
Received 19 June 2018; Received in revised form 20 September 2018; Accepted 11 November 2018
Available online 14 November 2018

Table 1
Baseline characteristics.

Number of patients	100
Age (years)	64.0 (27.8–82.1)
Male gender, n (%)	59 (59.0%)
Body mass index (kg/m^2)	23.7 (14.6–33.7)
Duration of atrial fibrillation (months)	9.0 (0.3–168.0)
Paroxysmal atrial fibrillation, n (%)	78 (78.0%)
CHA_2DS_2-VASc score	1 (0–6)
Left atrial diameter (mm)	37.0 (24.2–49.4)
Left atrial volume (cm^3)	90.3 (53.8–179.5)
Left ventricular ejection fraction (%)	66.7 (52.4–78.3)
Antiarrhythmic drug use, n (%)	49 (49.0%)

Values are the median (range) or the number of patients (%).
The CHA_2DS_2-VASc score is a clinical estimation of the risk of stroke in patients with atrial fibrillation; scores range from 0 to 9, with higher scores indicating a greater risk of stroke.

for noninferiority).[6] However, CB ablation requires more extensive fluoroscopic guidance to position the balloon catheter in the PVs. We hypothesized that anatomical factors of proximal PVs related to success of CB ablation. The purpose of our study was to investigate the anatomical features related to the success or failure of CB ablation for AF on pre-procedural cardiac computed tomography (CT) images.

2. Methods

This retrospective study was approved by our institutional review board; informed patient consent for the analyses was waived.

2.1. Study population

Our retrospective study included 123 consecutive patients with drug-refractory paroxysmal or persistent AF who had undergone cardiac CT between June 2016 and April 2017 for the evaluation of their left atrium (LA)- and the PV anatomy prior to the first CB ablation. AF was diagnosed by a cardiologist with 25 years of experience based on established guidelines.[9] Paroxysmal AF was defined as “AF that self-terminates within 7 days of onset”, persistent AF as “persistent AF lasting more than 7 days”. Inclusion criteria were patients who underwent contrast-enhanced cardiac CT. Our exclusion criteria were severe renal failure (estimated glomerular filtration rate < 45 ml/min/1.73 m^2, 17 patients), a history of hypersensitivity to iodinated contrast medium (3 patients) or pregnancy. Also excluded were another 3 patients with a right or left common PV canal because a large-diameter PV ostium could be an independent detrimental factor in CB ablation.[10,11] Thus, the final study population consisted of 100 patients (400 PVs); their baseline characteristics are summarized in Table 1.

2.2. Computed tomography (CT) scanning

All patients were scanned on a 64-detector row CT scanner (LightSpeed VCT; GE Healthcare, Milwaukee, WI, USA); retrospective ECG-triggered helical scans were performed. The scan and reconstruction parameters were tube voltage, 80 kVp; tube current, 100–675 mA; beam width, 40 mm; detector collimation, 64 × 0.625 mm; pitch factor, 0.16 or 0.2 mm/rotation; gantry rotation, 0.35 s; slice thickness, 0.625 mm; scan field of view (FOV), 320 mm; display FOV, 200 mm; matrix, 512 × 512; reconstruction, half; reconstruction kernel, standard; reconstruction method, filter back projection. Images were reconstructed starting from early systole (10% of R-R interval) and ending at end-diastole (90% of R-R interval) using 5% steps. An 70–80% phase location corresponding to atrial end-diastole was selected for image reconstruction in patients who were in sinus rhythm at the time of imaging.[12,13] If the patients had ongoing AF at the time of CT scan, a 50% phase location was selected for image reconstruction because it yielded the best image quality.[14] All scans were from the tracheal bifurcation to the level of the inferior margin of the cardiac apex in the craniocaudal direction. All patients were able to perform breath-holds during the examination. To evaluate coronary artery disease simultaneously, each patient was given nitroglycerin sublingually (0.3 mg) 5 min before scanning; patients whose heart rate exceeded 65 beats per minute thereafter additionally received landiolol hydrochloride (Corebeta; Ono Pharmaceutical Co., Ltd., Osaka, Japan).

We injected contrast medium (iodine concentration 350 mg/ml; Iomeron-350; Eisai, Tokyo, Japan) through a 20-gauge catheter into the antecubital vein using a power injector (Dual Shot type GX; Nemoto Kyorindo, Tokyo, Japan). The administered iodine dose was 245 mg/kg body weight. The injection volume was body weight × 0.7 ml administered in 14 s and followed by 20 ml of saline solution delivered at the same injection speed. The scanning delay was determined using a bolus-tracking method. A round, approximately 400 mm^2 region of interest (ROI) was placed in the center of the LA. Scanning was started manually 5 s after contrast enhancement exceeded a predefined threshold of 150 Hounsfield Units (HU).

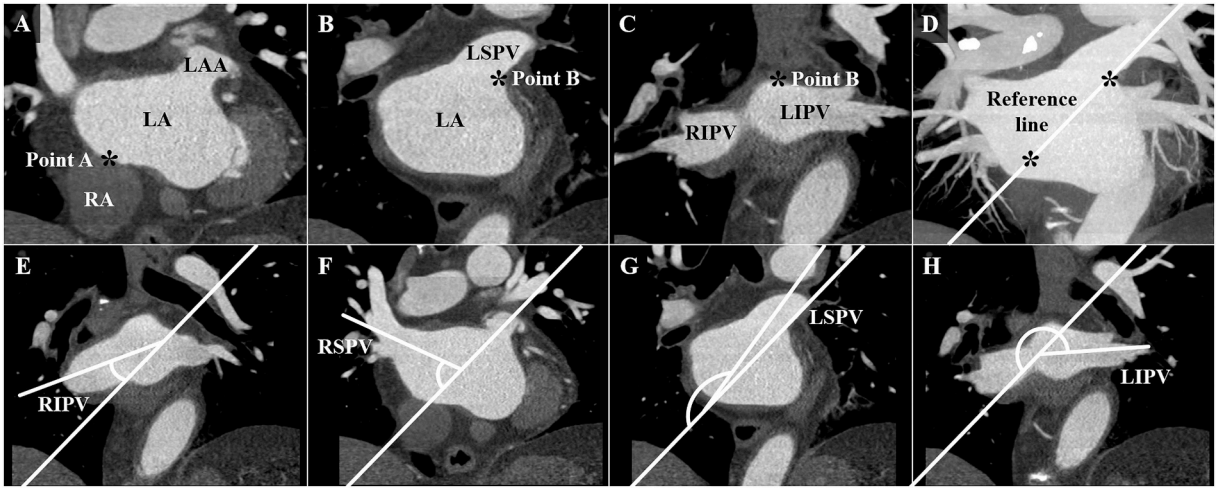

Fig. 1. Our process for measuring the PV angle. (A) A landmark (asterisk) is placed on the center of the atrial septum (point A). (B, C) Another landmark (asterisk) is placed at the center of the left PV from the bottom of the LSPV and the roof of LIPV (point B). (D) The line connecting points A and B is our reference line. (E–H) The angles of the RIPV, RSPV, LSPV and LIPV are obtained from the reference line and each PV ostium. LA, left atrium; LAA, left atrial appendage; RA, right atrium; LSPV, left superior pulmonary vein; LIPV left inferior pulmonary vein; RIPV, right inferior pulmonary vein; RSPV, right superior pulmonary vein.

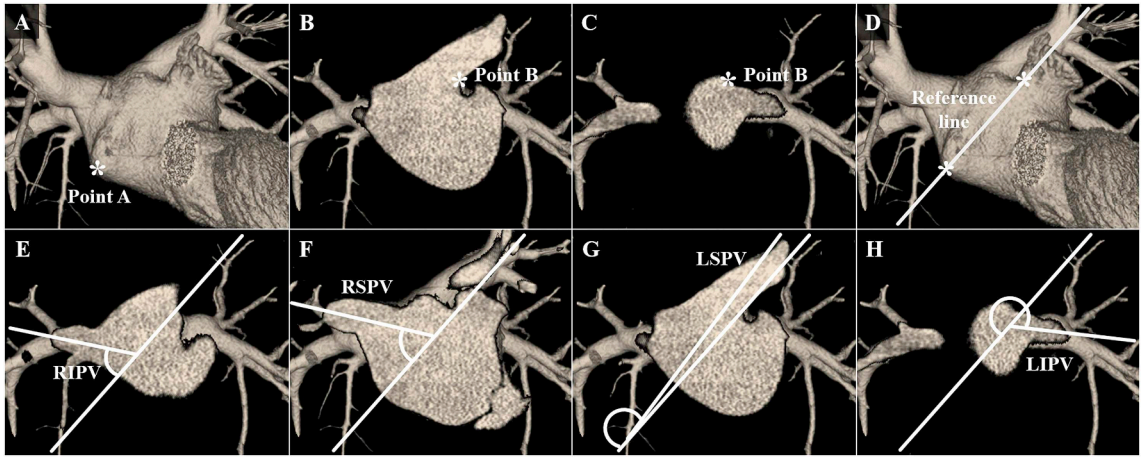

Fig. 2. 3D reconstructed images (anteroposterior direction) detailing our PV angle measurement process. (A) A landmark (asterisk) is placed at the center of the atrial septum (point A). (B, C) Another landmark (asterisk) is placed at the center between the bottom of the LSPV and the roof of the LIPV (point B). (D) The line connecting points A and B is our reference line. (E–H) The angles of the RIPV, RSPV, LSPV and LIPV are obtained from the reference line and each PV ostium. LSPV, left superior pulmonary vein; LIPV left inferior pulmonary vein; RIPV, right inferior pulmonary vein; RSPV, right superior pulmonary vein.

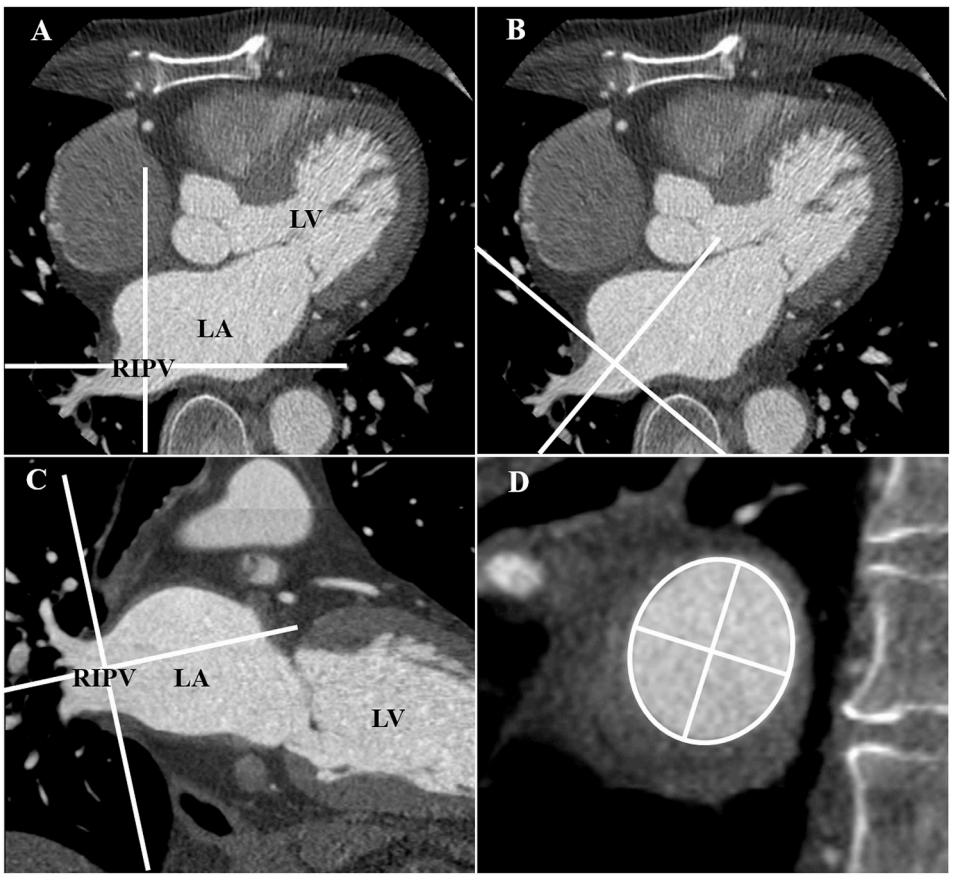

Fig. 3. Our process for measuring the short- and long length, the area, and the ovality of the RIPV ostium. (A) Crosshairs are placed in the RIPV ostial on the axial image. (B) The crosshair is rotated parallel to the RIPV ostium. (C) The crosshair is rotated parallel to the RIPV ostium on the oblique coronal image. (D) A cross-section orthogonal to the RIPV ostium is acquired. LV, left ventricle; LA, left atrium; RIPV, right inferior pulmonary vein.

2.3. Quantitative evaluation

Using multiplanar reconstruction (MPR) images obtained by pre-procedural cardiac CT, we measured 5 features of the ostium anatomy of each PV, i.e. its angle, short- and long axis length, area, and ovality[15,16] on a CT workstation (Advantage workstation ver. 4.4; GE Healthcare). All images were analyzed by two radiological technologists (Y.M. and T.M., with 13 and 15 years of experience with cardiac CT studies, respectively). They were blinded to the outcome of the clinical procedures and analyzed the CT images independently.

The PV angle was measured on coronal images as shown in Fig. 1A–H. The center of the atrial septum was defined as point A (Fig. 1A), the midpoint between the left superior- and left inferior PV (LSPV and LIPV) as point B (Fig. 1B and C). The line connecting points A and B was defined as the “reference line” (Fig. 1D) because the catheter tip was usually located at the midpoint between the LSPV and LIPV after catheter-puncture of the atrial septum during CB ablation. Then we measured the angle between the reference line and each PV (Fig. 1E–H). For a better understanding of our measurement process, 3-dimensional (3D) reconstructed images demonstrating our PV angle measurement are shown in Fig. 2A–H. Among our 100 patients there were no anatomical variants such as an accessory PV. Even in subjects

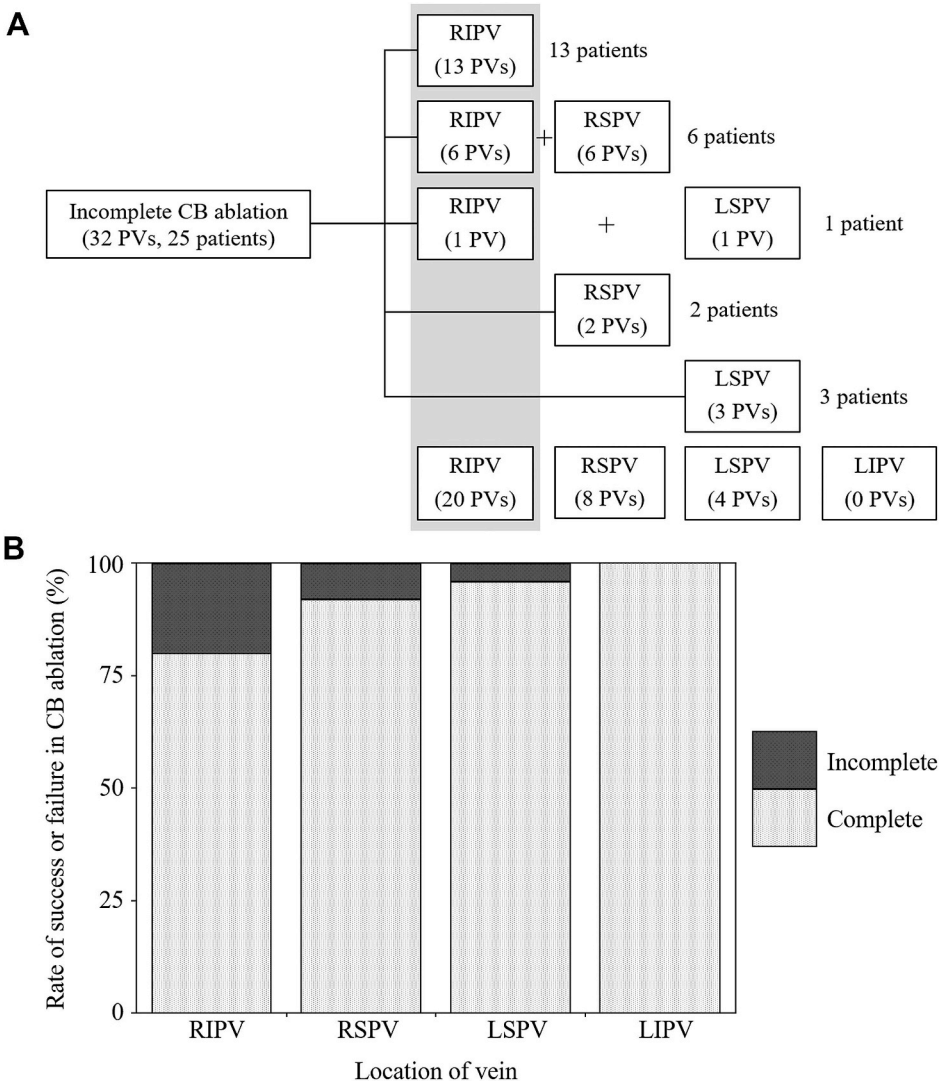

Fig. 4. Detailed procedural Results for CB ablation (400 PVs, 100 patients). (A) Breakdown of incomplete CB ablations (32 PVs, 25 patients); 20 RIPVs (20 patients) required touch-up ablation with RF, as did 8 RSPVs (8 patients) and 4 LSPVs (4 patients). (B) The rate of incomplete CB ablation was 20% for RIPVs, 8% for RSPVs, and 4% for LSVPs. All LIPVs were successfully ablated. RIPV, right inferior pulmonary vein; RSPV, right superior pulmonary vein; LSPV, left superior pulmonary vein; LIPV left inferior pulmonary vein.

Table 2
The distribution of the 5 anatomical features of interest in the 400 PVs.

	RIPV	RSPV	LSPV	LIPV	*p*-value
Angle (degree)	48.3 (18.4–77.7)	81.9 (56.2–110.1)	163.5 (142.2–175.1)	242.6 (209.8–267.6)	< 0.001
Short axis length (mm)	12.8 (6.3–19.9)	14.0 (7.3–22.0)	14.0 (8.0–21.6)	9.9 (2.8–20.0)	< 0.001
Long axis length (mm)	17.9 (12.3–25.7)	21.5 (14.4–29.5)	20.6 (14.6–28.5)	17.7 (11.5–22.9)	< 0.001
Area (mm^2)	178.0 (89.0–428.0)	230.5 (90.0–486.0)	218.0 (127.0–461.0)	134.5 (57.0–371.0)	< 0.001
Ovality	0.3 (0.0–0.9)	0.4 (0.0–1.1)	0.3 (0.0–0.9)	0.5 (0.1–1.2)	< 0.001

Values are the median (range).

with a right or left middle PV, our method allows measurements by using the reference line. We defined the PV ostium as the visual intersection of the PVs and the LA, determined by an inflection between the LA- and the PV wall.[17] The diameter of the short- and long axis length and the area of each PVs ostium was recorded as described elsewhere.[18–22] Fig. 3A - 3D show our measurement process at the right inferior PV (RIPV) ostium. We first placed a cross-hair in the RIPV ostium on axial images (Fig. 3A), obtained an oblique coronal image by rotating the cross-hair parallel to the RIPV (Fig. 3B), and then obtained an orthogonal cross-section by rotating the cross-hair vertically to the RIPV ostium on the oblique coronal image (Fig. 3C). The resulting image yielded the best view of the PV ostium and could be used to measure the diameter of the short- and long axis length and of the area (Fig. 3D).[12] Finally, we measured the diameter of the short- and long-axis length and of the area of the PV ostium on the workstation. Ovality was defined as the degree of deviation from perfect circularity and the value was expressed as 2 × [(long axis length) - (short axis length)]/[(long axis length + short axis length)].[15,16]

To investigate inter- and intraobserver variability in the quantitative measurements we performed Bland-Altman plot analysis for

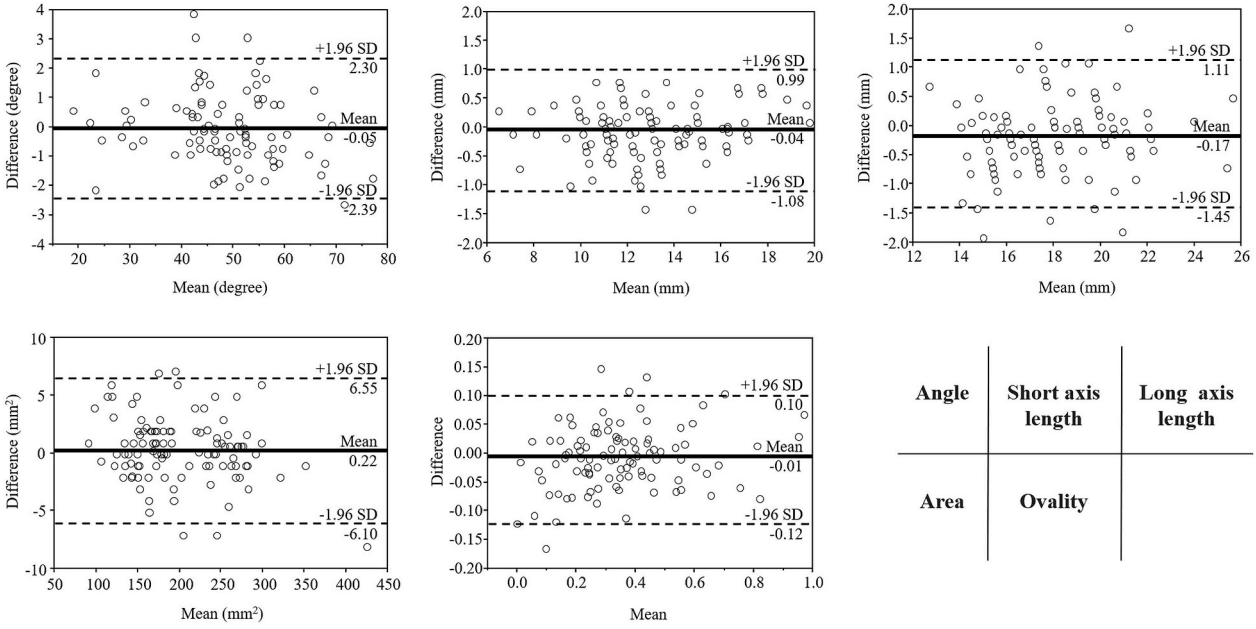

Fig. 5. Interobserver agreement in the quantitative evaluation of the RIPV (Bland-Altman plot analysis). The solid line represents the mean difference and the dashed lines represent the 95% limits of agreement (mean difference ± 1.96 SD). SD = standard deviations.

specific sites on 100 datasets (one dataset for each patient). To assess intraobserver agreement and to minimize recall bias, after a 2-week interval, each case was independently reanalyzed by the observers.

To avoid the potential effect of contrast enhancement, image quality, and especially of banding artifacts on the quantitative measurements of the PV parameters, we recorded the CT number and image noise [standard deviation (SD) of the CT number] in a circular ROI placed in the center of the LA and the epicardial fat on axial images. The size of the circular ROI cursors was as large as allowed by the LA diameter (approximately 5.0–10.0 mm^2) and by epicardial fat (approximately 1.5–3.0 mm^2). Based on the values obtained, we also calculated the contrast-to-noise ratio (CNR) using the formula:

CT number (LA) - CT number (epicardial fat)/image noise (LA).[23]

We also recorded the number of patients whose images were compromised by banding artifacts and assessed their effect on the quantitative measurement of our PV parameters.

2.4. CB ablation procedure

Two cardiologists (Y.M. and S.M., with 25 and 17 years of experience with catheter ablation, respectively) alternately performed all CB ablations during the period covered in this study.

Ablation was performed with the patients under deep sedation. An 9-Fr intracardiac echocardiography catheter (ViewFlex Xtra, Abbott, St. Paul, MN, USA) was introduced through the femoral vein and positioned in the right atrium. A 20-polar electrode catheter (BeeAT, Japan Lifeline, Tokyo, Japan) was placed in the coronary sinus. Double transseptal puncture was performed using an RF needle (Japan Lifeline) guided by both intracardiac echocardiography and fluoroscopy. After gaining LA access, a 100 UI/kg intravenous heparin bolus was injected. A steerable 15-Fr over-the-wire sheath (FlexCath, Medtronic, Minneapolis, MN, USA) was positioned in the LA. A circular mapping catheter (Achieve, Medtronic) was then advanced into each PV ostium. A 28-mm CB (Arctic Front Advance, Medtronic) was advanced over the wire up to the LA, inflated, and positioned in each PV ostium. Optimal vessel occlusion was defined by selective PV angiography showing total contrast retention with no backflow into the LA.

After complete occlusion was confirmed, we proceeded to the delivery of cryothermal energy. The ablation sequence was LSPV-LIPV-RIPV-right superior PV (RSPV). Our target temperature was −45 °C to −50 °C within 180 s.

During ablation of right-sided PVs, a decapolar catheter in the right ventricle was moved into the brachiocephalic vein and used to capture the diaphragm to warn of phrenic nerve injury. Phrenic nerve capture was monitored by tactile feedback of diaphragmatic contraction and assessment of the right diaphragmatic compound motor action potential. Ablation was terminated when the operator recognized a significant reduction in the compound motor action potential vis-à-vis the baseline. Amplitude variations dictated the application of the double-stop technique.

2.5. Determination of complete- and incomplete CB ablation

The primary outcome was defined as the establishment of a bidirectional block between the LA and PV, verified with a circular mapping catheter. When PV isolation was not achieved despite a total of 3 CB applications per vessel, we resorted to “touch-up” ablation with a conventional RF catheter (FlexAbility, Abbott) until isolation was confirmed. We recorded “complete CB ablation” when PV isolation was achieved with CB ablation alone, and “incomplete CB ablation” when CB plus RF ablation were required.

2.6. Statistical analysis

Continuous variables were expressed as the median and range, or as percentages or counts, as appropriate.

The rate of incomplete CB ablation between right-sided and left-sided PVs was assessed with the x^2-test. As the level of expertise with CB ablation may play a role in the success of the intervention, we also compared the procedural outcomes using the x^2-test. Analysis of variance was used to determine the distribution of the 5 features of interest among the PVs. Inter- and intraobserver agreement by Bland-Altman plot analysis was expected to converge to a 95% limits of agreement, defined as a mean difference of ± 1.96 SD. Univariable and

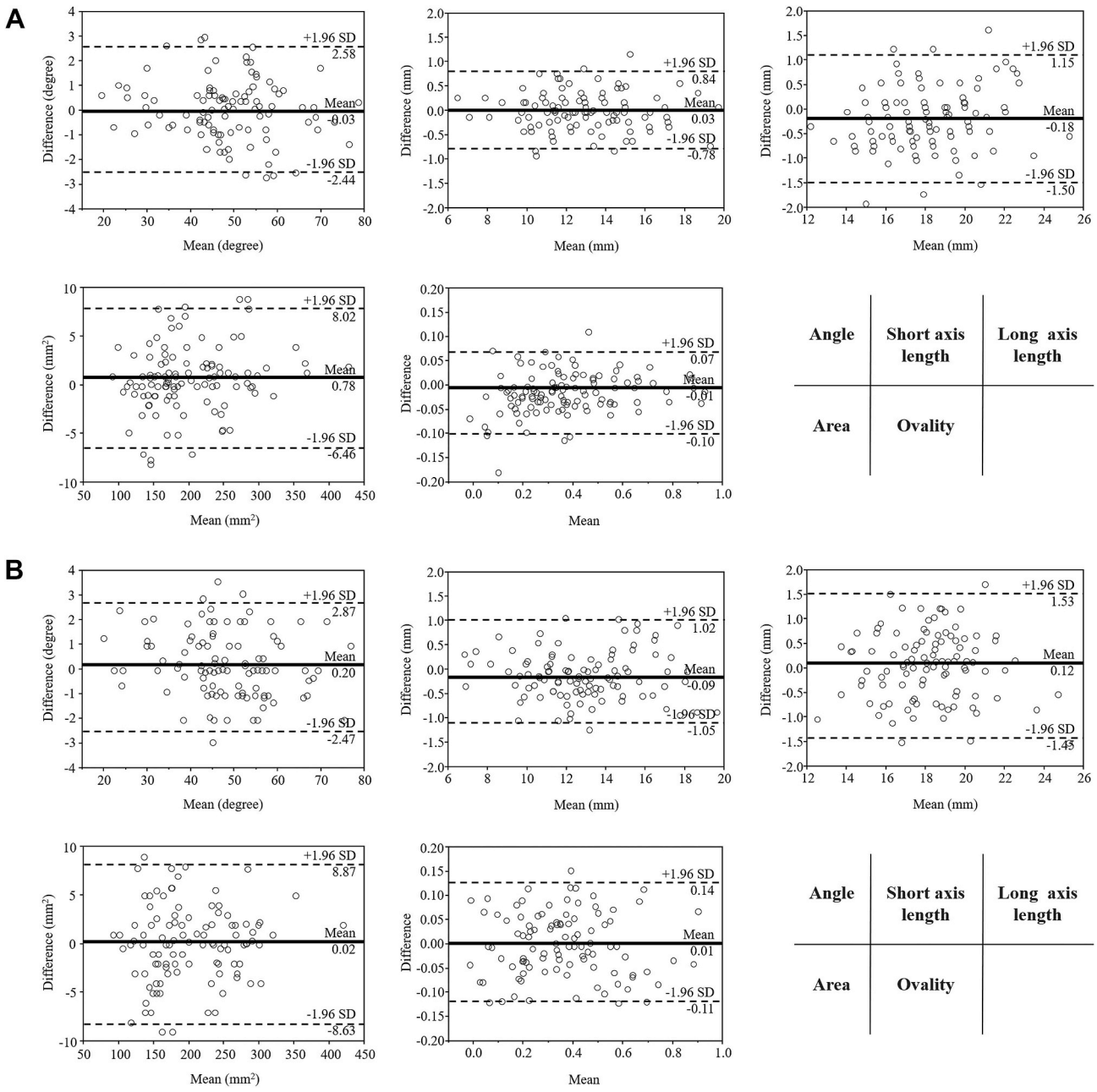

Fig. 6. Intraobserver agreement in the quantitative evaluation of the RIPV (Bland-Altman plot analysis). (A) Observer 1 (B) Observer 2 The solid line represents the mean difference and the dashed lines represent the 95% limits of agreement (mean difference ± 1.96 SD). SD = standard deviations.

Table 3
Results of univariate and multivariate logistic regression analyses of the effect of the 5 anatomical features of interest on incomplete CB ablation in the RIPV.

Predictor	Univariate analysis				Multivariate analysis[a]			
	OR	95%CI		*p*-value	AOR	95%CI		*p*-value
Angle	1.17	1.09	1.26	< 0.0001	1.17	1.09	1.27	< 0.0001
Short axis length	0.89	0.74	1.07	0.2136	–			
Long axis length	0.84	0.69	1.02	0.0784	0.86	0.69	1.09	0.2136
Area	0.99	0.98	1.00	0.0842	–			
Ovality	1.36	0.10	18.39	0.8158	0.56	0.02	14.69	0.7313

$R^2 = 0.33$, $p < 0.0001$, $n = 400$.
AOR, Adjusted odds ratio.
[a] Multivariate logistic regression with stepwize method ($p < 0.25$).

Table 4
Results of univariate and multivariate logistic regression analyses of the effect of the 5 anatomical features of interest on incomplete CB ablation in the RSPV.

Predictor	Univariate analysis				Multivariate analysis[a]			
	OR	95%CI		*p*-value	AOR	95%CI		*p*-value
Angle	1.09	1.01	1.19	0.0244	1.12	1.01	1.23	0.0136
Short axis length	0.97	0.79	1.19	0.7737	–			
Long axis length	0.86	0.70	1.05	0.1342	0.94	0.75	1.17	0.5573
Area	1.00	0.99	1.00	0.4712	–			
Ovality	0.24	0.01	8.32	0.4424	0.03	0.00	3.31	0.1357

$R^2 = 0.15$, $p = 0.03$, $n = 400$.
AOR, Adjusted odds ratio.
[a] Multivariate logistic regression with stepwize method ($p < 0.25$).

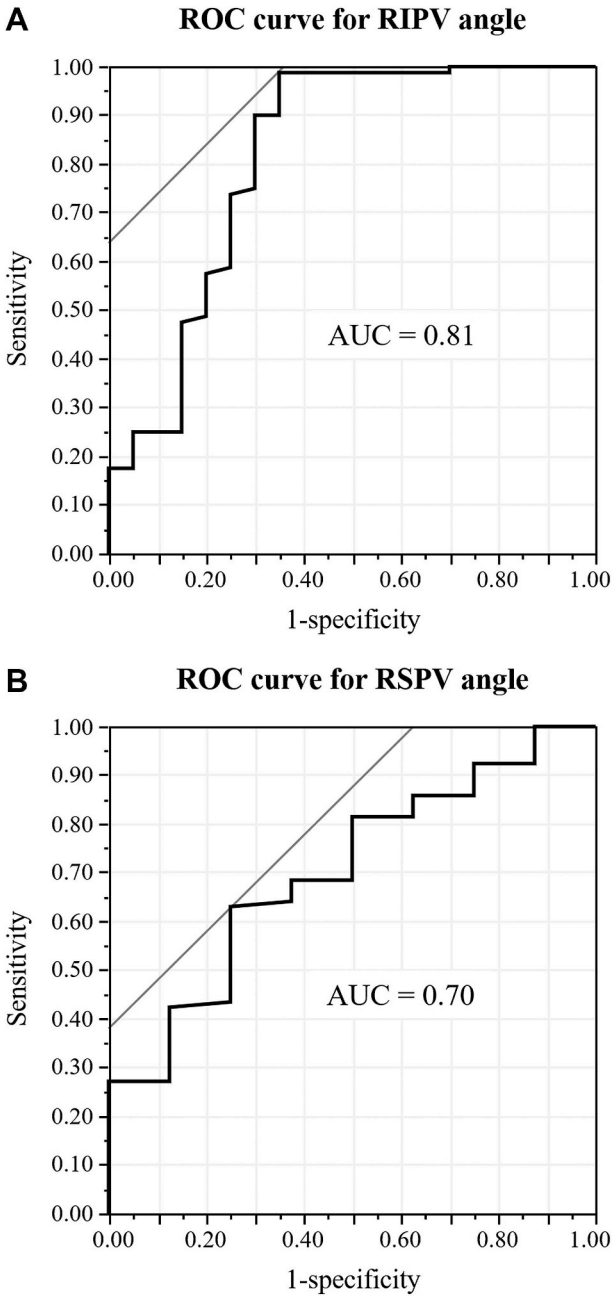

Fig. 7. ROC analysis of incomplete CB ablation and PV angles. (C)RIPV angle cut-off of 40.1° discriminated an incomplete CB ablation with a sensitivity of 99% and specificity of 65%. (D) RSPV angle cut-off of 79.7° discriminated an incomplete CB ablation with a sensitivity of 63% and specificity of 75%. RIPV, right inferior pulmonary vein; RSPV, right superior pulmonary vein; ROC, receiver-operating characteristic; AUC, area under the curve.

multivariable logistic regression analysis was conducted for each PV to investigate the relationship between incomplete CB ablation and the 5 features of interest. Incomplete or complete CB ablations were the outcome variables; the explanatory variables were the angle, the short- and long-axis length, and the area and ovality of the PVs. For multivariable logistic regression analysis we selected variables by the stepwise method. A p-value < 0.25 was the criterion for variable selection. We performed a receiver-operating characteristic (ROC) curve analysis to identify an appropriate cut-off value for anatomical features significantly associated with incomplete CB ablation. All statistical analyses were performed with JMP 14 (SAS Institute Inc., Cary, NC, USA). Differences of $p < 0.05$ were considered statistically significant.

3. Results

3.1. Procedural results

The outcome of CB ablation addressing 400 PVs in 100 patients was retrospectively evaluated. Incomplete ablation was recorded for 32 PVs (8%) in 25 patients (Fig. 4A, 4B). Of these, 13 patients (17 PVs) were treated between 5 months; the other 12 patients (15 PVs) underwent the procedure between 6 months. There was no significant difference in the rate of incomplete CB ablation between the two periods ($p = 0.857$). "Touch-up" ablation adding RF ablation was required to treat 20 RIPVs in 20 patients (RIPV, n = 13; RIPV plus RSPV, n = 6; RIPV plus LSPV, n = 1); in 12 patients a superior PVs underwent "touch-up" ablation (RSPV, n = 8; LSPV, n = 4). All LIPVs (n = 100) were successfully CB-ablated.

The rate of incomplete CB ablation was significantly higher for right-than left-sided PVs (right-sided PVs, 28%; left-sided PVs, 4%; $p < 0.001$).

3.2. Measurement of the major PVs on pre-procedural cardiac CT images

The distribution of the 5 anatomical features of interest in the 400 PVs is summarized in Table 2; there were significant inter-vessel differences in the PV angle, short- and long-axis length, area, and ovality (all features, $p < 0.001$). The angle in particular tended to depend on the PV location. The time required to measure the PV angles in each patient was about 5 min.

Bland-Altman plots for inter- and intraobserver agreement with respect to the RIPV in our 100 datasets are summarized in Figs. 5 and 6. The plots nearly converged within the 95% limits of agreement for all anatomical features.

On pre-procedural cardiac CT images, the median CT number for the LA was 505.0 HU (range, 269.0–794.3 HU). The SD for epicardial fat was 40.5 (range, 28.1–51.2). The CNR at these sites was 15.2 (range, 9.2–27.3). Banding artifacts were observed in 19 of the 100 patients. While they did not affect the reference line in 10 of these patients, they had an effect on measurements of the ostium of the RIPV (n = 2), RSPV (n = 4), LSPV (n = 1), and LIPV (n = 2).

3.3. Relationship between incomplete CB ablation and anatomical features

Univariate logistic regression analysis showed that the PV angle was significantly associated with incomplete CB ablation of right-sided PVs. For multivariate logistic analysis of the RIPV and RSPV we applied the angle, the long-axis length, and PV ovality in a stepwise method. We again found that the angle was significantly associated with incomplete CB ablation of right-sided PVs [adjusted odds ratio (AOR) = 1.17; 95% confidence interval (CI): 1.09–1.27, $p < 0.001$; AOR = 1.12, 95% CI = 1.01–1.23; $p = 0.014$ for the RIPV and RSPV, respectively) (Tables 3 and 4).

In the ROC analysis, the Az value and the optimal cut-off value for RIPV angle to discriminate an incomplete CB ablation were 0.81 and 40.1°, respectively. The diagnostic ability of the cut-off value was sensitivity of 99% and specificity of 65% (Fig. 7A). The Az value and the optimal cut-off value for RSPV angle to discriminate an incomplete CB ablation were 0.70 and 79.7°, respectively. The diagnostic ability of the cut-off value was sensitivity of 63% and specificity of 75% (Fig. 7B). In patients with PV angles predicting incomplete CB ablation, the touch-up ablation was required in 13/14 (93%) and 6/40 (15%) patients at the RIPV and RSPV, respectively.

Representative cases of complete- and incomplete CB ablation at the RIPV angle are shown in Fig. 8. In case 1 with complete CB ablation (Fig. 8A), the measured RIPV angle on the CT image was 77.8°; it was 24.2° in case 2 with incomplete ablation (Fig. 8B). Fluoroscopic imaging performed during CB ablation showed that the catheter angle reflected the vessel angle in both cases (Fig. 8C and D).

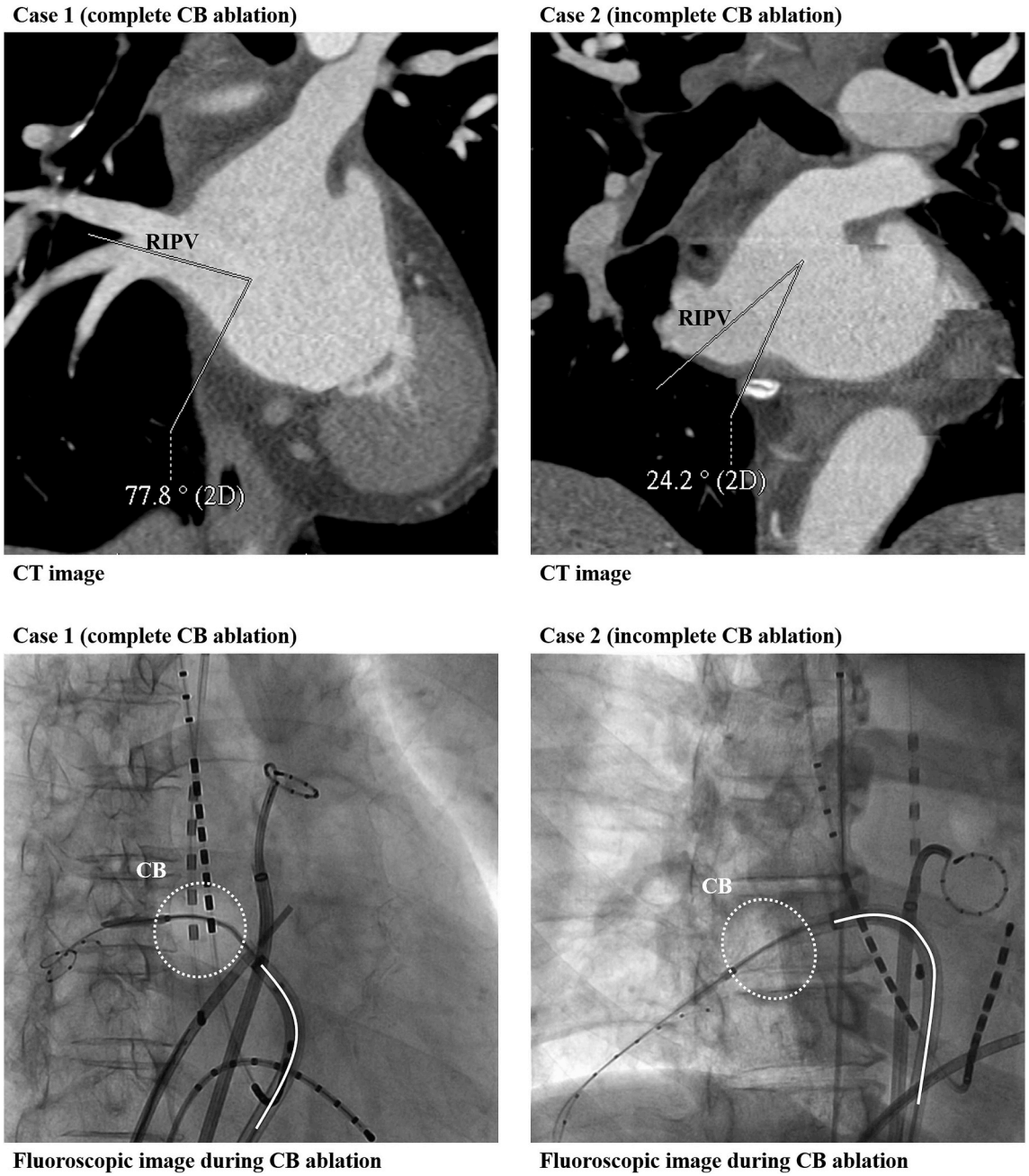

Fig. 8. Representative cases with complete- (case 1) and incomplete (case 2) CB ablation. (A, B) MPR images derived from original CT images. The RIPV angle was 77.8° in case 1 (A) and 24.2° in case 2 (B). (C, D) Fluoroscopic images (30° right anterior oblique view) obtained during CB ablation of the RIPV. On the fluoroscopic image of case 1 (C), the catheter forms a gentle curve. Complete PV isolation was obtained due to good adhesion between the CB and the RIPV ostium and CB ablation was successful. In case 2 (D), the catheter curve was steep and adhesion between the CB and the RIPV ostium was inadequate. CB ablation was incomplete. RIPV, right inferior pulmonary vein; CB; cryoballoon.

4. Discussion

We examined pre-procedural cardiac CT scans of 100 patients with paroxysmal or persistent AF who had undergone a first CB ablation at our institution. We found that the rate of incomplete CB ablation was significantly higher for the RIPV among other major PVs and that the anatomical feature significantly associated with incomplete CB ablation was the vessel angle. In our series of 400 PVs, 368 (92%) were successfully ablated after PV isolation.

Others[12,15,16] reported that anatomical PV features such as an oval shape, early branching, and a dull-edged shape were associated with difficult maneuvers during CB ablation and that the PV angle affected PV isolation and played a role in the success or failure of CB ablation.[13,15] However, the earlier reports failed to describe the method by which the angle was measured. To obtain reproducible, objective angle measurements, we placed a reference line that connected the center of the atrial septum with the midpoint between the LSPV and the LIPV.

Our findings are comparable to those of earlier studies.[8,24–27] Successful PV isolation for CB ablation may require a sufficiently low temperature for good adhesion between the PV ostium and the balloon.[10,11] Anatomically, the RIPV ostium and fossa ovalis, the puncture site, are located on adjacent sides of the same site. Schmidt et al.,[20] who evaluated the mean distance between the fossa ovalis and 4 PVs on magnetic resonance imaging scans, found that it was shortest to the

RIPV. Consequently, catheter manipulation to the RIPV may be more difficult than to other major PVs.[13] We confirmed that good adhesion of the balloon to the vessel ostium is particularly difficult when the RIPV angle is small (Fig. 8). To obtain good adhesion, it may be advisable to place the puncture at the lower side of the atrial septum, to adjust the depth of the sheath, or to change the branch for the indwelling wire. However, a small RIPV angle complicates complete CB ablation and touch-up ablation with RF must be performed.

Our findings show that anatomical features, i.e. the short- and long axis length, and the PV area and ovality, were not-while the PV angle was associated with incomplete CB ablation. We encountered few instances of incomplete CB ablation of left-sided PVs although others[12,28] reported that due to their ovality, it was difficult to isolate left PVs. Ang et al.[28] cited CB freezes, their duration, and the lowest obtainable temperature as factors that rendered vessel isolation and CB ablation difficult. Although we did not consider procedural details in our definition of complete and incomplete CB ablation, our findings are similar to theirs. Ovality is a factor related to incomplete CB ablation of left PVs, and further detailed analyses may be necessary.

Although others[12,28] reported that ovality was a significant factor related to incomplete CB ablation, in our series it was not. In the earlier studies 23- or 28-mm CBs were used; we introduced only 28-mm CBs. We hypothesize that good adhesion can be obtained by inserting 28-mm CBs even when the PV ostium is oval.

To examine the reproducibility of our quantitative measurements we performed Bland-Altman plot analysis. We found that with respect to all studied anatomical features, our measurements were reproducible and inter- and intraobserver agreement was high. Therefore we think that anatomical measurements at major PVs are reliable for predicting the success or failure of CB ablation.

The quantitative measurement of PV parameters might be moderately affected by contrast enhancement, the image quality, and especially by banding artifacts. We found that the image quality did not affect quantitative measurements of the PVs. Although a low image quality and especially banding artifacts are encountered on images acquired on 64-detector row CT scanners, these disadvantages can be addressed by iterative reconstruction and by using wide-detector CT scanners.

Pre-procedural cardiac CT studies are essential for morphological- and thrombus evaluations and for 3D electroanatomical mapping systems[29]; their careful quantitative analysis may facilitate the selection of appropriate ablation strategies (CB- or RF ablation). The addition of anatomical measurements may help further to predict difficulties in PV isolation and contribute to reducing the cost of CB ablation and the burden on patients and operators.

Our study has some limitations. It was a single institution, retrospective study on Japanese patients whose body habitus is different from that of North Americans and Europeans, and our findings reflect the skill and experience of the operator. Therefore, multi-center studies that include large patient populations are needed to confirm our findings. Also, as the use of our technique was not approved before June 2016, we cannot present long-term outcomes. In future studies we will address the relationship of the PV anatomy and long-term treatment Results by identifying the site of PV-LA reconnection. Lastly, there might be a statistical issue with respect to multiple observations on individual patients.[30] Individuals generally harbor 4 PVs, and numerical variables such as the PV angles may be correlated. To address this issue, multiple measurement of individual variables should be recorded for each patient although ethical considerations prevent the acquisition of multiple cardiac CT scans for this purpose. Consequently, the results of our multivariate logistic regression analysis may be over-stated.

5. Conclusions

In conclusion, our analysis demonstrates that the rate of incomplete CB ablation was significantly higher for right-than left-sided PVs and that the PV angle was an anatomical feature significantly associated with incomplete CB ablation. Anatomical information obtained on pre-procedural cardiac CT scans is useful for selecting CB ablation strategies and for predicting the treatment outcome.

Disclosures

The authors have no conflicts of interest directly relevant to the content of this article.

References

1. Go AS, Hylek EM, Phillips KA, et al. Prevalence of diagnosed atrial fibrillation in adults: national implications for rhythm management and stroke prevention: the AnTicoagulation and Risk Factors in Atrial Fibrillation (ATRIA) Study. *J Am Med Assoc.* 2001;285:2370–2375.
2. Fang MC, Go AS, Chang Y, et al. Comparison of risk stratification schemes to predict thromboembolism in people with nonvalvular atrial fibrillation. *J Am Coll Cardiol.* 2008;51:810–815.
3. Wang TJ, Larson MG, Levy D, et al. Temporal relations of atrial fibrillation and congestive heart failure and their joint influence on mortality: the Framingham Heart Study. *Circulation.* 2003;107:2920–2925.
4. Bertaglia E, Stabile G, Senatore G, et al. Documentation of pulmonary vein isolation improves long term efficacy of persistent atrial fibrillation catheter ablation. *Int J Cardiol.* 2014;171:174–178.
5. Natale A, Raviele A, Arentz T, et al. Venice Chart international consensus document on atrial fibrillation ablation. *J Cardiovasc Electrophysiol.* 2007;18:560–580.
6. Kuck KH, Brugada J, Furnkranz A, et al. Cryoballoon or radiofrequency ablation for paroxysmal atrial fibrillation. *N Engl J Med.* 2016;374:2235–2245.
7. Boho A, Misikova S, Spurny P, et al. Complications of circumferential pulmonary vein isolation using the cryoballoon technique: incidence and predictors. *Int J Cardiol.* 2014;171:217–223.
8. Kojodjojo P, O'Neill MD, Lim PB, et al. Pulmonary venous isolation by antral ablation with a large cryoballoon for treatment of paroxysmal and persistent atrial fibrillation: medium-term outcomes and non-randomised comparison with pulmonary venous isolation by radiofrequency ablation. *Heart.* 2010;96:1379–1384.
9. Fuster V, Ryden LE, Cannom DS, et al. ACC/AHA/ESC 2006 guidelines for the management of patients with atrial fibrillation: a report of the American college of cardiology/American heart association task force on practice guidelines and the European society of cardiology committee for practice guidelines (writing committee to revise the 2001 guidelines for the management of patients with atrial fibrillation): developed in collaboration with the european heart rhythm association and the heart rhythm society. *Circulation.* 2006;114:e257–354.
10. Sarabanda AV, Bunch TJ, Johnson SB, et al. Efficacy and safety of circumferential pulmonary vein isolation using a novel cryothermal balloon ablation system. *J Am Coll Cardiol.* 2005;46:1902–1912.
11. Chun KR, Furnkranz A, Schmidt B, et al. Right ventricular rapid pacing in catheter ablation of atrial fibrillation: a novel application for cryoballoon pulmonary vein isolation. *Clin Res Cardiol.* 2009;98:493–500.
12. Sorgente A, Chierchia GB, de Asmundis C, et al. Pulmonary vein ostium shape and orientation as possible predictors of occlusion in patients with drug-refractory paroxysmal atrial fibrillation undergoing cryoballoon ablation. *Europace.* 2011;13:205–212.
13. Yasuoka R, Kurita T, Kotake Y, et al. Particular morphology of inferior pulmonary veins and difficulty of cryoballoon ablation in patients with paroxysmal atrial fibrillation. *Circ J.* 2017;81:668–674.
14. Dong J, Dalal D, Scherr D, et al. Impact of heart rhythm status on registration accuracy of the left atrium for catheter ablation of atrial fibrillation. *J Cardiovasc Electrophysiol.* 2007;18:1269–1276.
15. Knecht S, Kuhne M, Altmann D, et al. Anatomical predictors for acute and mid-term success of cryoballoon ablation of atrial fibrillation using the 28 mm balloon. *J Cardiovasc Electrophysiol.* 2013;24:132–138.
16. Schmidt M, Dorwarth U, Straube F, et al. Cryoballoon in AF ablation: impact of PV ovality on AF recurrence. *Int J Cardiol.* 2013;167:114–120.
17. Kato R, Lickfett L, Meininger G, et al. Pulmonary vein anatomy in patients undergoing catheter ablation of atrial fibrillation: lessons learned by use of magnetic resonance imaging. *Circulation.* 2003;107:2004–2010.
18. Jongbloed MR, Dirksen MS, Bax JJ, et al. Atrial fibrillation: multi-detector row CT of pulmonary vein anatomy prior to radiofrequency catheter ablation–initial experience. *Radiology.* 2005;234:702–709.

19. Mansour M, Holmvang G, Sosnovik D, et al. Assessment of pulmonary vein anatomic variability by magnetic resonance imaging: implications for catheter ablation techniques for atrial fibrillation. *J Cardiovasc Electrophysiol.* 2004;15:387–393.
20. Schmidt B, Ernst S, Ouyang F, et al. External and endoluminal analysis of left atrial anatomy and the pulmonary veins in three-dimensional reconstructions of magnetic resonance angiography: the full insight from inside. *J Cardiovasc Electrophysiol.* 2006;17:957–964.
21. Schwartzman D, Lacomis J, Wigginton WG. Characterization of left atrium and distal pulmonary vein morphology using multidimensional computed tomography. *J Am Coll Cardiol.* 2003;41:1349–1357.
22. Wood MA, Wittkamp M, Henry D, et al. A comparison of pulmonary vein ostial anatomy by computerized tomography, echocardiography, and venography in patients with atrial fibrillation having radiofrequency catheter ablation. *Am J Cardiol.* 2004;93:49–53.
23. Gupta AK, Nelson RC, Johnson GA, Paulson EK, Delong DM, Yoshizumi TT. Optimization of eight-element multi-detector row helical CT technology for evaluation of the abdomen. *Radiology.* 2003;227:739–745.
24. Van Belle Y, Janse P, Rivero-Ayerza MJ, et al. Pulmonary vein isolation using an occluding cryoballoon for circumferential ablation: feasibility, complications, and short-term outcome. *Eur Heart J.* 2007;28:2231–2237.
25. Klein G, Oswald H, Gardiwal A, et al. Efficacy of pulmonary vein isolation by cryoballoon ablation in patients with paroxysmal atrial fibrillation. *Heart Rhythm.* 2008;5:802–806.
26. Chun KR, Schmidt B, Metzner A, et al. The 'single big cryoballoon' technique for acute pulmonary vein isolation in patients with paroxysmal atrial fibrillation: a prospective observational single centre study. *Eur Heart J.* 2009;30:699–709.
27. Okumura K, Matsumoto K, Kobayashi Y, et al. Safety and efficacy of cryoballoon ablation for paroxysmal atrial fibrillation in Japan- results from the Japanese prospective post-market surveillance study. *Circ J.* 2016;80:1744–1749.
28. Ang R, Hunter RJ, Baker V, et al. Pulmonary vein measurements on pre-procedural CT/MR imaging can predict difficult pulmonary vein isolation and phrenic nerve injury during cryoballoon ablation for paroxysmal atrial fibrillation. *Int J Cardiol.* 2015;195:253–258.
29. Steinberg BA, Hammill BG, Daubert JP, et al. Periprocedural imaging and outcomes after catheter ablation of atrial fibrillation. *Heart.* 2014;100:1871–1877.
30. Gonen M, Panageas KS, Larson SM. Statistical issues in analysis of diagnostic imaging experiments with multiple observations per patient. *Radiology.* 2001;221:763–767.